Combination of CRISPR and LASER ART Eliminates Replication Competent Rebound in Humanized Mice

Kamel Khalili[1] and Howard E. Gendelman[2]

1. Department of Neuroscience, Center for Neurovirology, Comprehensive NeuroAIDS Center, Lewis Katz School of Medicine at Temple University, Philadelphia, PA
2. Department of Pharmacology and Experimental Neuroscience, University of Nebraska, Omaha, NE

ABSTRACT

BACKGROUND: Advances in CRISPR-Cas9gene editing technology and its in vivo delivery by AAV9 vectors together with cell based nanotechnology for long-acting slow effective release antiretroviral therapy (LASER-ART), were used in NSG-CD34 humanized mice to facilitate eradication of HIV-1 in vivo.

METHODS: CRISPR-Cas9 proviral DNA excision followed two months of treatment with long-acting slow effective release antiretroviral therapy (LASER-ART), rilpivirine, myristolyated dolutegravir, lamivudine, and abacavir in HIV-1 infected humanized mice. A series of virological, histological, and DNA and RNA assays were used to detect HIV-1 expression and replication in the animal tissues. Ultra deep, whole genome sequencng was employed to assess in vivo off-target effects.

RESULTS: Results from three independent sets of studies showed restorations of CD4+ T cells due to ART treatment and complete eradication of replication competent virus by CRISPR in 39% of animals. Ultrasensitive nested and digital droplet PCR and RNA scope assays failed to detect HIV-1 in blood, spleen, lung, kidney, liver, gut-associated lymphoid tissue and brain. Excision of proviral DNA fragments spanning the LTRs and the Gag gene from the integrated proviral DNA was identified, while no off target effects were observed. The absence of viral rebound following cessation of ART with no progeny virus recovery after in vivo adoptive transfer of human immunocytes from dual-treated virus-free animals to uninfected humanized mice verified HIV-1 eradication by the combined treatment strategy. In contrast, HIV-1 was readily detected in all infected animals treated with LASER ART or CRISPR-Cas9 alone.

CONCLUSIONS: The sequential application of LASER ART and CRISPR-Cas9 therapies administered to HIV-1 infected humanized mice provides the first proof-of-concept that viral sterilization is possible.

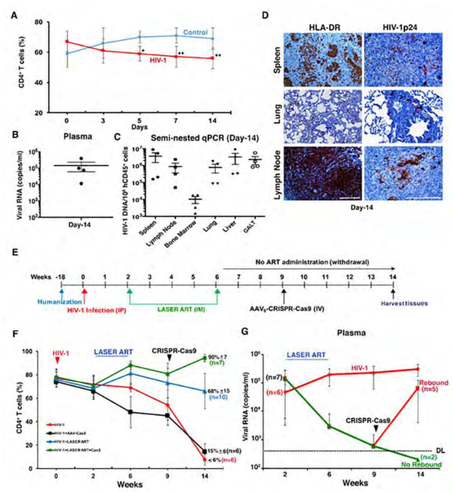


Figure 1. Viral and immune profiles following sequential LASER ART and AAV_9-CRISPR-Cas9 treatments of HIV-1 infected NSG-humanized mice. (A) Human CD4+ T cells (%) in mice were enumerated by flow cytometry tests on days 0, 3, 5, 7, and 14 post-infection in HIV-1 infected animals (red line). Uninfected control animals are shown by the blue line. **(B)** Representative data of virus in blood (plasma viral RNA copies/ml) are shown 14 days after HIV-1 infection (n=4). **(C)** HIV-1 DNA was observed by semi-nested real-time qPCR in tissues of all HIV-1 infected animals 14 days after viral infection (n=4). **(D)** Representative data sets of human HLA-DR in lymph nodes, spleen and lung demonstrating significant human cell reconstitution in all animals. Tissue sections stained for HIV-1p24 readily show large numbers of infected cells in tissues at day-14. **(E)** The study scheme illustrates time points of infection and treatment. After confirmation for the establishment of the viral infection (shown in A-D) the rest 29 replicate humanized mice were subdivided into four groups. The first group (n=6) of mice were left untreated (HIV-1 control), the 2nd group (n=6) received a single intravenous dose of AAV_9-CRISPR-Cas9 (10^{12} GC units), nine weeks post-infection, the 3rd group (n=10) were administered LASER ART by intramuscular injection after two weeks of viral infection, the 4th (n=7) were given LASER ART (week 2-6 as in group 3) and three weeks after the last LASER ART treatment, a single intravenous dose of AAV_9-CRISPR-Cas9 (as in group-2). All mice remained without additional ART treatment for an additional five weeks. **(F)** Flow cytometry tests of human CD4+ T cells are shown with increased numbers in the LASER ART and LASER ART+AAV_9-CRISPR-Cas9 group. **(G)** Evaluation of viral load indicated that after administration of AAV_9-CRISPR-Cas9, two out of seven mice showed no evidence for viral rebound at 14 weeks. Viral load in untreated animals remained high during the course of study. One-way ANOVA and Bonferroni's post-hoc tests for multiple comparisons and two-tailed Student's *t-test* were used for statistical analyses in A. $^*P < 0.05$, $^{**}P<0.01$.

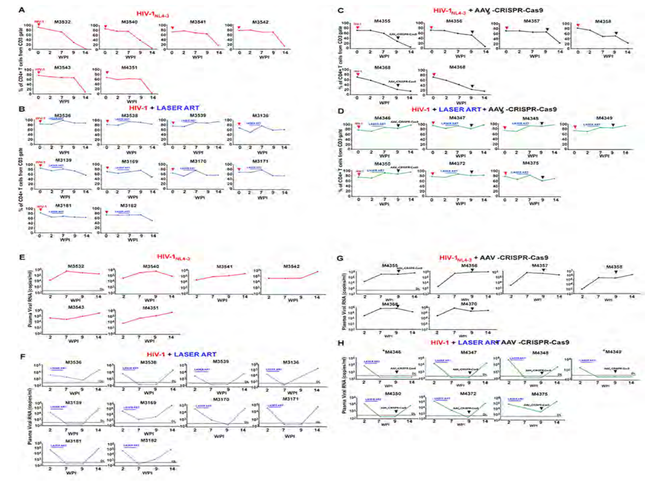


Figure 2. Flow cytometric evaluation of human CD4+ T cells and Viral loads in individual humanized mice for HIV-1_{NL4-3} infected and/or treated groups. (A-D) Peripheral blood of CD34-NSG-humanized mice were assayed before and after (2, 7, 9, and 14 weeks post HIV-1 infection (WPI) for the presence of human CD4+ cells from CD3+ gated populations throughout the study. **(A)** Percentage of human CD4+ T cells followed a decreased pattern in all mice in the HIV-1 infected group. **(B)** CD4+ T cell profile of HIV-1 + LASER ART animals showed a decline in percentage of CD4+ T cells after two weeks of infection, after which the LASER ART treatment was followed for four additional weeks and the mice were then allowed for eight additional weeks without ART. **(C)** Percentage of human CD4+ T cells were decreased in all mice in the HIV-1 and AAV_9-CRISPR-Cas9 infected group. **(D)** CD4+ T cells of HIV-1 + LASER ART + AAV_9-CRISPR-Cas9 animals. Decreased percentages of CD4+ T cells were seen as early as two weeks of infection in all mice, after which the LASER ART treatment was administered for four weeks followed by AAV_9-CRISPR-Cas9 injection given at week-9. The mice were then followed for an additional five weeks. **(E-H)** Plasma viral load of CD34+ NSG-hu mice was assayed after weeks 2, 7, 9, and 14 of HIV-1 infection for HIV-1 RNA to assess progression of disease using COBAS Amplirep-Taqman-48 V2.0, the sensitivity of the assay after adjustment to dilution factor is (200 copies/ml). **(E)** VL of six HIV-1 infected mice. **(F)** VL profile of HIV-1+LASER ART animals. We observed a rebound of viral RNA at the study end in all 10 LASER ART treated animals, which corresponds to eight weeks after therapy interruption. **(G)** VL of all six HIV-1 infected +AAV_9-CRISPR-Cas9 group. **(H)** VL profile of HIV-1 + LASER ART + AAV_9-CRISPR-Cas9 animals (n=7). Rebound of viral RNA was observed at the study end in five of seven dual treated animals, which corresponds to eight weeks-post therapy interruption, but observed no virus in two dual treated animals (#4346 and 4349).

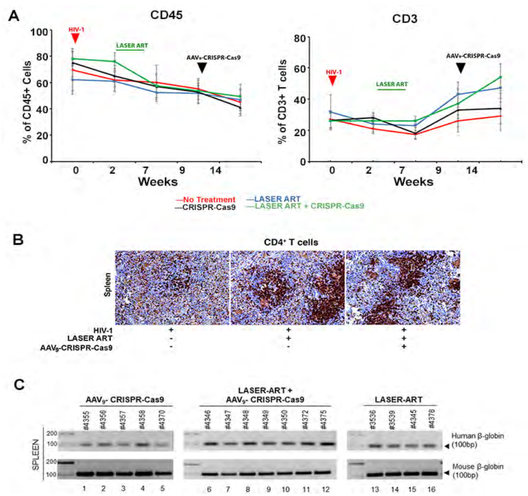


Figure 3. Flow cytometric evaluations of human leukocyte reconstitution in blood and spleen of humanized mice. **(A)** Peripheral blood of HSC reconstituted mice was assayed before and after (weeks 2, 7, 9, and 14) HIV-1 infection for the presence of human CD45+ (Left Panel) and CD3+ (Right Panel) cells. These experiments were performed to assess levels of humanization and percentage of total T cells (CD3 population) throughout the study. These included animals, group-1, HIV-1 infected (n=6), group-2, HIV-1 and CRISPR Cas9 (n=6), group-3, HIV-1 and LASER ART (n=10) and group-4, HIV-1 and LASER ART and CRISPRCas9 (n=7). Notably, in the HIV-1 infected mice group, the numbers of CD45+ and CD3+ human cells in blood of mice were comparable to each of the treatment groups. The colored triangles in the top identify the treatment time points during study (red-HIV-1 infection (no treatment, blue is LASER ART alone, black is CRISPR-Cas9 and green is LASER ART and CRISPR Cas9 injection to respective mice groups. We did not observe any statistically difference in any of the time points as compared to control animals. **(B)** IHC of spleens from HIV-1 infected humanized mice. To determine the presence of human target T cells, spleens from HIV-1_{NL4-3} infected animals (untreated, LASER ART or both LASER ART +CRISPR/Cas9) were assessed for the presence of CD4+ T cells. Significant reductions in CD4+ T cells numbers (brown stained cells) are readily seen in the HIV-1-infected group compared to HIV-1 infected animals treated with LASER ART with/without CRISPR-Cas9. **(C)** Verification of the presence of human cells in the spleens of humanized mice. PCR analysis of genomic DNA isolated from the spleens of humanized mice using primer sets specific to human and mouse (for a control) beta-globin genes.

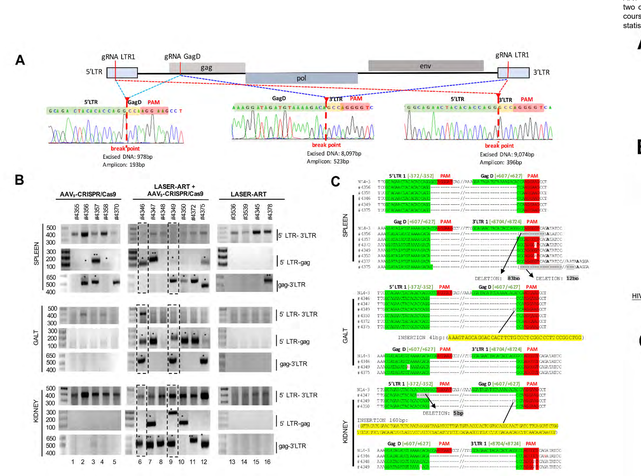


Figure 4. Excision of the viral DNA fragments by CRISPR-Cas9 in tissues from HIV-1 infected humanized mice treated with LASER ART. (A) Schematic illustration of HIV-1_{NL4-3} DNA highlighting the positions of gRNA LTR1 and gRNA GagD target sites, their nucleotide compositions, and the three possible CRISPR-Cas9 induced break points leading to the excisions of various lengths of viral DNA fragments. **(B)** Total DNA from spleen, GALT, and kidney from three groups of animals used for PCR genotyping with a set of primers derived from the 5'LTR, 3'LTR, and gag gene. Reaction conditions were calibrated for efficient amplification of short (less than 600 bp) or large DNA fragments. Predicted amplicons of 193 bp and 523 bp, which result from the excisions of DNA fragments between 5'LTR to Gag and Gag to 3'LTR, respectively, were selected for DNA sequencing. The fragment of 396 bp represents both populations of full length LTRs, as well as the chimeric of both 5' and 3'LTR after excision of entire genome by gRNA LTR1/CasB and re-joining of residual segments of cleaved 5'LTR and 3'LTRs. Several other fragments with similar size, caused by InDel mutations, were detected and further analyzed by sequencing. Single asterisks above the bands point to the specificity of fragmental HIV DNA excision by CRISPR-Cas9 as verified by Sanger sequencing (also illustrated in figs. S5 and S6). The double asterisk depicts non-specific amplification of unrelated DNA or randomly amplified segmental truncated HIV-1 sequence (also see fig. S7). The dashed boxes show the excision of expected DNA fragments of the HIV-1 genome in the two animals with no viral rebound. **(C)** Representative DNA sequences from each group were aligned to the reference LTR-Gag region of the HIV-1_{NL4-3} sequence. The positions and nucleotide compositions of targets for gRNAs LTR1 and GagD are shown in green, PAM in red, and insertion sequences in yellow. Arrows highlight positions of small and large deletions.

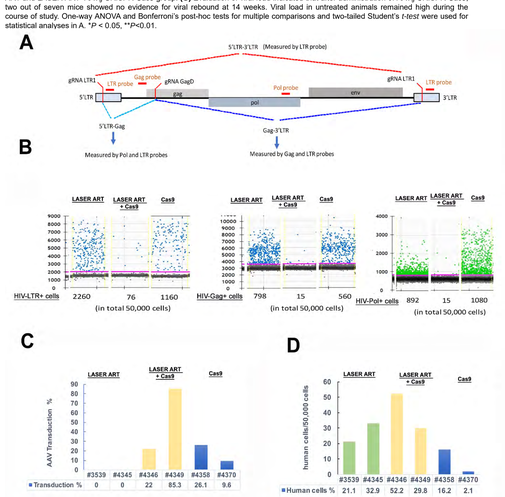


Figure 5. Efficiency of the proviral DNA excision by CRISPR-Cas9. (A) Schematic of the locations of each gRNA and TaqMan probe and the possible excision outcomes. **(B)** Absolute quantification of HIV-infected cells detected by digital-droplet PCR (ddPCR) using indicated primers and probes targeting LTR, Gag and Pol, respectively. Representative data collected from one HIV-infected humanized mouse of each group treated with LASER-ART (ART), LASER-ART plus CRISPR/Cas9 (ART/Cas9) or CRISPR/Cas9 only (Cas9). The genomic DNA extracted from a total of 50,000 cells including human and mouse cells was used as template for each ddPCR analysis. As shown in Panel A, the reduction of Gag presents a deletion between 5'LTR and Gag or 5'LTR to 3'LTR, while a reduction in Pol represents the excision between Gag to 3'LTR or 5'LTR to 3'LTR. However, a single LTR will always remain to be detectable in all three conditions. Thus, we can use the ratio of Gag or Pol to LTR to estimate the excision efficiency. For example, in mouse #4349, the ratios of Gag/LTR and Pol/LTR are 19.7% (17 cells with detectable gag out of 76 cells with detectable LTR) and 19.4%, respectively, in the genomic DNA extracted from the spleen of the treated mice. Thus, the excision efficiencies of 5'LTR to Gag and Gag to 3'LTR were estimated to be about 80% for both (1 minus 19.7% or 100% - 19.4%). In the spleen of the same mouse, the AAV9 transduction efficiency was calculated as high as 85% of the total population including both human graft and mouse host cells. In another mouse #4346, we demonstrated that the excision occurred mainly in Gag to 3'LTR because the ratio of Pol/LTR is 38.4% while Gag/LTR is 89.4%. Thus, the excision efficiency was estimated at 61.6% in 5'LTR to Gag and 10.6% in Gag to 3'LTR. Nonetheless, the presence of 2 LTRs in an uncut HIV proviral DNA was not considered in order to simplify the estimate. **(C)** TaqMan probe and primers specific for saCas9, which was delivered by AAV9, were used to determine the AAV transduction efficiency and represented as the percentage of the cells containing saCas9 in a total of 50,000 cells including both human and mouse cell populations. **(D)** Total human cell population in these 50,000 cells was measured using TaqMan probe and primers specific for human b-actin.

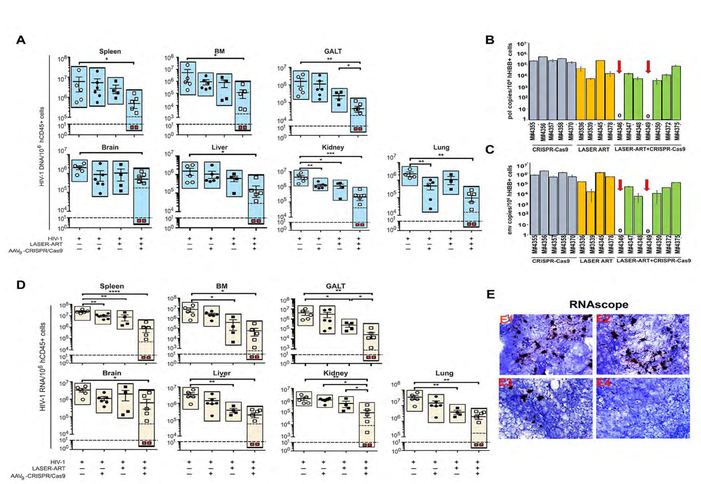


Figure 6. Detection of viral DNA and RNA at endpoint in various tissues after sequential LASER ART and AAV_9-CRISPR-Cas9 treatments in infected humanized mice. (A) HIV-1 DNA and **(D)** HIV-1 RNA analyses using ultrasensitive semi-nested real-time qPCR assays from spleen, bone marrow (BM), GALT, brain, liver, kidney, and lung from treatment groups described in Figure 1F-G. The data represent each of the four groups: HIV-1 infected controls (n=5), HIV-1 infected and AAV_9-CRISPR-Cas9 treated (n=6), HIV-1 infected and LASER ART treated alone (n=4) and HIV-1 infected LASER ART and AAV_9-CRISPR-Cas9 treated mice (n=7). The data are expressed as total HIV-1 DNA **(A)** or HIV-1 RNA **(D)** copies/10^6 human CD45+ cells. Two animals, #4346 and #4349 [shown by the red squares below the dashed lines (detection limit)], with dual treatments, showed sterilization of virus from all tissues analyzed. **(B and C)** Quantitative PCR showed complete elimination of signals corresponding to *pol* **(B)** and *env* **(C)** DNA sequences of HIV-1 in mice #4346 and #4349 (shown by red arrows). **(E)** Representative results from RNAscope assay revealed the detection of single or clusters of brown dots corresponding to HIV-1 RNA in 5 µm-thick spleen sections of infected animals receiving either LASER ART or CRISPR-Cas9 alone, but not both (#4346). *E1*, humanized mice infected with HIV-1 (controls); *E2*, HIV-1 infected animals treated only with CRISPR-Cas9; *E3*, HIV-1 infected LASER ART treated animals demonstrating viral rebound after cessation of therapy; *E4*, infected animals treated first with LASER ART followed by CRISPR-Cas9. *E1-E4* are representative tissue sections taken from each of the animal groups. In these assays, we used the antisense V-HIV1-Clade-B targeting 854-829bp of HIV-1 as the probe. Images are 40x magnification. One-way ANOVA and Bonferroni's post-hoc tests for multiple comparisons and two-tailed Student's *t-test* were used for comparisons between two groups as in A and D for statistical analyses. $^*P < 0.05$, $^{**}P < 0.01$, $^{***}P <0.001$.

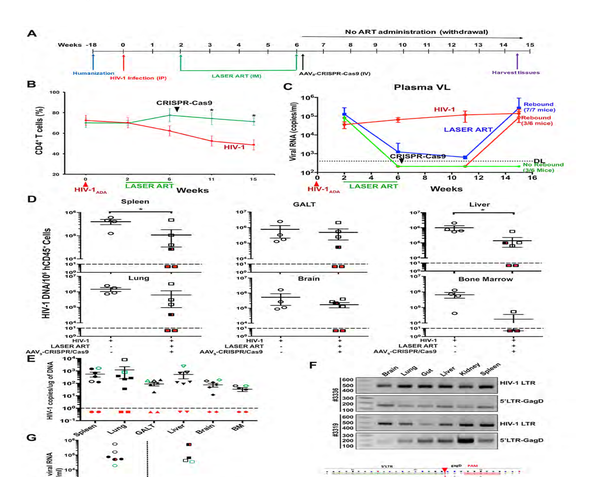


Figure 7. Viral sterilization in HIV-1_{ADA} infected humanized mice by LASER ART and CRISPR-Cas9 (dual treated) validated by viral, immune and excision profiling. (A) The timeline of the experiment showing the temporal administration of LASER ART and CRISPR-Cas9 treatments, and animal sacrifice. **(B)** The percentage of human CD4+ T cells and **(C)** viral loads measured in the HIV-1 infected (n=4), HIV-1 infected and LASER ART alone (n=7) and HIV-1 infected and dual treated (n=6) animal groups. Dual treated animals (n=6) that showed no (n=3) or viral rebound (n=3) in plasma are illustrated. **(D)** HIV-1 DNA analysis was performed using ultrasensitive semi-nested real-time qPCR assays from spleen, GALT, liver, lung, brain and bone marrow from infected (n=4) and infected and dual treated mice (n=6). Three animals from the dual treated rebound group had very few bone marrow cells. Therefore, the data represented in n=3 for the dual treated animals in the BM adoptive transfer studies. The data are expressed as total HIV-1 DNA copies/10^6 human CD45+ cells. Two animals, #3319 and #3336 (illustrated by the red squares) were below the dashed lines for virus detection as measured by plasma VL. These animals had no detectable viral DNA after dual treatments demonstrating viral sterilization from all analyzed tissues. A single animal (#3324), as illustrated by a half-red-dashed line, had an undetectable VL in plasma, but viral DNA was amplified in all the tissues analyzed. **(E)** Ultrasensitive ddPCR, with sensitivity of detecting 1-2 viral copies, was used in cross validation tests for viral DNA detection and performed in tissues of infected and infected/dual treated animals. As a positive control, one animal each from the HIV-1 infected (open black structure) and HIV-1 and LASER ART (open green structure) groups are illustrated together. These were placed together with the six infected animals from the dual treatment group to show the presence of segments of HIV-1 LTR DNA and detection of a 121 bp amplicon, indicative of excision of a DNA fragment between the LTR and the *gag* gene (top). The histogram illustrates representative results from sequencing of the 121 bp fragment highlighting the position of the 5' LTR breakpoint, and Gag and PAM trinucleotide on the GagD RNA. (G) *An in vivo* viral outgrowth assay was performed by adoptive transfer of splenocytes and bone marrow cells from infected and "virus eradicated" LASER ART CRISPR Cas9-treated mice to uninfected recipient CD34+ NSG-hu mice. These animals failed to show viral recovery after one month of examination by plasma viral RNA measurements. In confirmation assays performed as positive controls two animals from an HIV-1 infected groups (shown by open black circles for spleen and boxes for bone marrow) and an animal from a LASER ART treatment group are shown as open green circles (spleen) and box (bone marrow). All controls readily recovered virus. Five animals from the dual treatment group are illustrated as closed circles (spleen) and boxes (bone marrow). Virus was not detected in plasma from animals injected with splenocytes and bone marrow cells isolated from 2 "dual-treated" animals (#3319 and #3336, red circles and boxes). This was used as the definition of viral eradication in these experiments. One animal each from the HIV-1 and dual treated bone marrow injected group died so their data was not included. One-way ANOVA and Bonferroni's post-hoc tests for multiple comparisons and two-tailed Student's *t-test* were used for comparisons between two groups as in B and D for statistical analyses. $^*P < 0.05$.

	HIV-1			LASER ART				CRISPR-Cas9					
Experiment	1st	2nd	3rd	1st	2nd	3rd	1st	2nd	3rd	1st	2nd	3rd
Mouse Numbers	6	6	7	10	2	5	7	6	10	6	NA	7
Viral Rebound*	6/6	4/4	7/7	10/10	2/2	5/5	5/7	3/6	6/10	6/6	NA	7/7

Table 1. Summary of viral rebound from three independent studies in three sets of HIV-1 infected CD34+ NSG-hu mice with single and combination treatments with LASER ART and/or CRISPR-Cas9.

*Plasma viral RNA copies of > 10^4 /ml
The viral strains used were HIV-1NL4-3 and HIV-1_{ADA} in the 1st and 2nd and 3rd experiments respectively.

Contributors

Prasanta K. Dash[1#], Rafal Kaminski[2#], Ramona Bella[2#], Hang Su[1], Saumi Mathews[1], Taha M. Ahooyi[2], Chen Chen[2], Pietro Mancuso[2], Rashan Sariyer[2], Pasquale Ferrante[2], Martina Donadoni[2], Jake A. Robinson[2], Brady Sillman[1], Zhiyi Lin[1], James R. Hilaire[1], Mary Banoub[1], Monalisha Elango[1], Nagsen Gautam[3], R. Lee Mosley[1], Larisa Y. Poluektova[1], JoEllyn McMillan[1], Aditya N. Bade[1], Santhi Gorantla[1], Ilker K. Sariyer[2], Tricia H. Burdo[2], Won-Bin Young[2], Shohreh Amini[2], Jennifer Gordon[2], Jeffrey M. Jacobson[2], Benson Edagwa[1], Kamel Khalili[2*], Howard E. Gendelman[1*]

[1]Department of Pharmacology and Experimental Neuroscience, University of Nebraska Medical Center, Omaha, NE 68198-5880 USA
[2]Department of Neuroscience, Lewis Katz School of Medicine at Temple University, Philadelphia, PA 19115 USA
[3]Department of Pharmaceutical Sciences, College of Pharmacy, University of Nebraska Medical Center, Omaha, NE 68198-5880 USA

[#]Equal contributions made

This work was made possible by grants awarded by the NIH to KK and HEG.

Conflict of interests:

KK is a named inventor on patents that cover the viral gene editing technology that is the subject of this article. HEG is a named inventor on patents that cover the medicinal and polymer chemistry technologies that were also employed in this manuscript. In addition to the foregoing interests, KK is a co-founder, board member, scientific advisor, and holds equity in Excision Biotherapeutics, a biotech start-up that has licensed the viral gene editing technology from Temple University for commercial development and clinical trials. HEG is the founder of Brain First a second independent biotech start-up and is the operative head of the Nebraska Nanomedicine Production Plant, a good manufacturing program facility that was responsible for synthesizing the long-acting slow effective release antiretroviral therapies used in the accompanying report. The authors declare that this work was produced solely by the authors and that no other individuals or entities influenced any aspects of the work including, but not limited to, the study conception and design; data acquisition, analysis and interpretation; and writing of the manuscript. No other entities provided funds for the work. The authors further declare that they have received no financial compensation from any other third parties for any aspects of the published work.